Potential Sputtering of Lithium Fluoride by Slow Multicharged Ions

T. Neidhart, F. Pichler, F. Aumayr, HP. Winter, M. Schmid, and P. Varga*

Institut für Allgemeine Physik, Technische Universität Wien, Wiedner Hauptstrasse, 8-10/134, A-1040 Wien, Austria

(Received 9 November 1994)

Thin polycrystalline LiF films have been bombarded by slow ($\leq$1 keV) multicharged Ar^{q+} ions ($q \leq 9$), in order to study the resulting total sputter yields by means of a quartz crystal microbalance. More than 99% of sputtered particles are neutral and show yields, at given impact energy, in proportion to the potential energy of projectile ions. The respective "potential sputtering" process already takes place far below 100 eV impact energy. It can be related to defect production in LiF following electron capture by the multicharged ions, and removes about one LiF molecule per 100 eV of projectile potential energy.

PACS numbers: 79.20.Rf, 79.20.Nc, 79.90.+b

Recently, Neidhart *et al.* [1] observed total sputter yields of about 0.5 LiF molecule per primary ion, for impact of rather slow ($\geq$5 eV) He^+, Ne^+, and Ar^+ ions on polycrystalline lithium fluoride. Since for metal surfaces no sputtering takes place at such low impact energies, this sputtering of LiF has been related to "electronic effects" initiated by electron transfer from the LiF surface into projectile ions. F^+ secondary ion yields resulting from impact of slow singly and doubly charged noble gas ions on LiF differ by more than 1 order of magnitude [2], which has been explained by the comparably more efficient Auger neutralization (AN) and/or resonance neutralization (RN) from the LiF valence band into doubly charged ions. Generally, for impact of slow multicharged ions (MCI) on alkali halide surfaces a rapid increase of the secondary ion yields with projectile charge q has been demonstrated [3]. When etching a KCl surface previously bombarded with slow Ar^{q+} or Kr^{q+} at given ion fluxes, higher charged ions turn out to cause larger etching patterns [4]. Based on such evidence, Bitenskii, Murakhmetov, and Parilis [5] have proposed a so-called "Coulomb explosion" sputter mechanism for insulators under slow MCI impact. Conceivably, this process should be initiated by the strong negative charge depletion in the uppermost target layers due to the rapid electron capture into incoming MCI, leaving behind positive target ion cores which then may push each other out of the solid. Sputtering of metals is exclusively caused by kinetic energy transfer from projectiles onto the target particles, producing nonthermal velocity distributions of sputtered particles with steeply decreasing yields below typically 500 eV impact energy [6]. Ion induced sputtering from alkali halides results in much slower (thermal) particle velocities, similarly as for electron and photon stimulated desorption (ESD and PSD) [7,8] from alkali halides. Only a small fraction shows comparably high velocities as for sputtering of metals. Most particles from ion induced sputtering of alkali halides are neutral [9], as for ESD and PSD. For the latter processes, recent studies [7,8] explain the observed, rather large neutral desorption yields by efficient creation of defects in the near surface region, which suggests that similar mechanisms may also account here for the interesting ion induced sputtering of LiF [1].

To investigate this in more detail, we have studied total sputtering yields for impact of multicharged ions on LiF. We used rather low impact energies to keep kinetic sputtering effects negligible, and the potential energy content of the MCI was partly much larger than their kinetic energy. Determination of the sputter yield has been performed by means of a quartz crystal microbalance technique [1]. Planoconvex SC-cut crystals have been coated on one side with a thin (300 nm) film of polycrystalline LiF by evaporation in high vacuum. The ion bombardment caused an increase of the crystal's resonance frequency as a direct measure of the LiF film mass loss. This technique does not suffer from the problems inherent to collection of sputtered particles (e.g., incompletely known collection geometry and/or neutral particle sticking coefficients), since the total sputter yields can be readily determined from the frequency change for known ion current density. High stability of the resonance frequency (approximately 1 mHz rms frequency noise at 6 MHz) was achieved by operating the quartz crystals within ± 0.1 °C of the minimum of their frequency vs. temperature curved at 150 °C and by keeping the LiF target at this temperature. Influence of thermal stress arising from temperature gradients due to the energy deposited by incoming ions has been strongly reduced by using SC-cut crystals [10], which have a resonance frequency insensitive to radial stress.

Ar^{q+} ions ($q \leq 9$) from a 5 GHz electron cyclotron resonance (ECR) source [11] were magnetically mass-to-charge separated into an ultrahigh vacuum (UHV) target chamber. A 3° kink in the ion beam line removed charge-exchanged neutral particles in front of an ion deceleration lens defining the final impact energy ($10 \leq E_k \leq 1000$ eV) on target. The lower limit in achievable impact energies was set by the ion source energy spread of typically $5 \times q$ eV. Homogeneous target irradiation was assured by ion beam scanning over the target surface. Experimental errors of the absolute

 0031-9007/95/74(26)/5280(4)$06.00

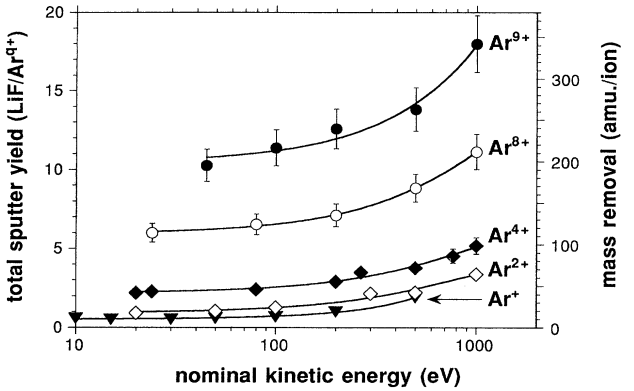

FIG. 1. Total sputter yield vs. projectile kinetic energy for different Ar^{q+} charge states q. The given yields refer to sputtered mass losses measured in units of LiF molecule masses. Experimental errors of typically ±10% as specified in the text are shown by error bars, if larger than the respective symbol size. Solid lines for guidance only.

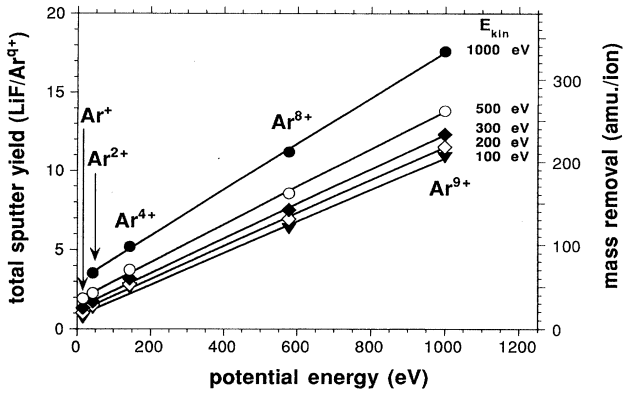

FIG. 2. Dependence of total LiF sputter yield on the MCI potential energy at different impact energies. Linear fits (solid straight lines) are in good agreement with the data points. Error bars as in Fig. 1, but here not shown for convenience.

total sputter yields Y resulted mainly from ion beam instabilities during individual sputter cycles and amounted to typically ±10%.

Thin LiF films evaporated on amorphous substrates show a polycrystalline structure with favored orientation of the LiF [111] axis normal to the substrate surface [12]. The present measurements have been performed on clean stoichiometric surfaces obtained by annealing after prolonged heating at 400 °C, as shown by secondary ion mass spectrometry (impurities less than 0.5% of the Li^+ and F^- signals). The stoichiometry was demonstrated by low energy ion scattering at target temperatures between 20 and 400 °C after annealing, in agreement with the behavior of LiF single crystals [13]. MCI current densities were kept below 10 nA/cm^2. Data were only taken after reaching an equilibrium for implanted Ar atom saturation with ion doses of typically 5×10^{14} ions/cm^2. Whereas LiF single crystals below 300 °C become charged up under ion impact, this was not the case for our thin LiF films at the rather low ion fluxes applied, as was demonstrated from temperature-independent yields of both scattered primary ions and the secondary ions.

The dependence of the measured total sputter yields Y on the projectile impact energy E_k has been plotted in Fig. 1 for different projectile charges. Toward higher E_k, Y increases gradually, while staying approximately constant below $E_k \approx 100$ eV. The clear influence of the projectile potential energy E_p, in direct relation with the ion charge state q, becomes apparent from Fig. 2, where the MCI kinetic energy has been corrected for image charge acceleration (see below). At low E_k, total sputter yields Y amount to typically one LiF molecule per 100 eV potential energy. The additionally measured electron-induced total sputtering yields [13] are shown versus electron impact energy in Fig. 3 (note that ESD from LiF at a target temperature below 150 °C removes only F^0 atoms, as will be discussed later). In the following, our results are explained by combining available knowledge on the neutralization of slow MCI on metal surfaces [14,15] with the now broadly accepted mechanisms responsible for ESD and PSD from alkali halides [7,8], and by consideration of recently measured MCI-induced slow electron yields from LiF [16].

The interaction of slow MCI with the valence electrons of a metal surface can be described be a classical over-barrier model [17]. The approaching MCI causes a collective electronic response of the solid, which can be simulated by the ion image charge. At low nominal impact energy and higher q, this image charge attraction considerably enhances the actual (effective) impact energy at the surface. As soon as the potential barrier between the surface conduction band and available empty projectile states has dropped below the Fermi level, classically allowed RN can take place and will rapidly form a so-called "hollow atom" [15]. Autoionization of this multiply excited complex gives rise to electron emission "above the surface." Inside the solid, the projectile is further neu-

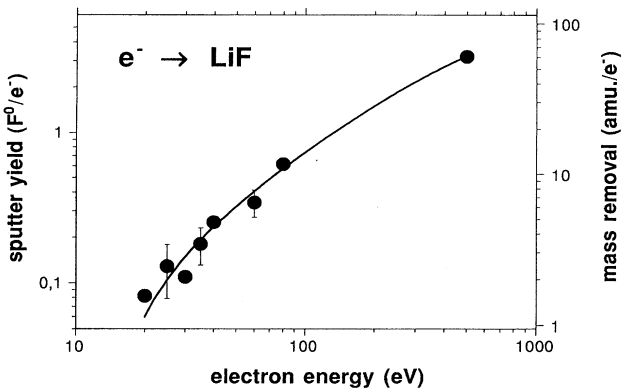

FIG. 3. Electron-induced sputter yields for F^0 atoms from LiF vs electron impact energy, from Neidhart *et al.* [13]. Solid line for guidance only.

tralized by resonant and quasiresonant neutralization and/or AN. Still present projectile inner shell vacancies decay by emission of fast Auger electrons. For a LiF surface, in contrast to a metallic one, the valence electron wave functions are more localized and the effective work function is considerably larger due to a large band gap [18]. Therefore, classically allowed RN may only start at comparably shorter distances from the surface, and the comparably immobile electrons of the F($2p$) valence band will probably not permit the formation of a hollow atom [19], as can be guessed from the considerably smaller electron yields for slow MCI impact on LiF [16] in comparison with clean gold [15]. In any case, neutralization and de-excitation processes taking place before, at, and below the LiF surface will produce holes in the F($2p$) valence band and also free electrons.

ESD and PSD of neutral particles from alkali halide surfaces [7,8] are initiated by creation of electron-hole pairs due to the impinging electrons or photons. Holes formed inside the F($2p$) valence band are called "hot holes" and can diffuse very rapidly until becoming trapped by impurities or by forming "V_k centers" (F_2^- molecular ions adjacent to two anion sites). These V_k centers can trap available electrons, thus forming "self-trapped excitons" [20], which at room temperature will immediately decay into two "color centers," i.e., a "H center" (F_2^- molecular ion at an anion lattice site) and a "F center" (electron localized at the next or second-next anion site). At the surface, H centers decay by emitting F^0 atoms and the F centers can neutralize Li^+ cations. The such created Li atoms at the surface can give rise to a metallic layer which at room temperature will stay on and stop further progress of ESD or PSD, but will be evaporated at temperatures above 150 °C.

We propose the following model for neutral particle desorption induced by hyperthermal MCI impact on LiF. If a highly charged ion approaches the LiF surface, holes in the F($2p$) valence band will be created by RN. These "cold holes" localized at the Fermi edge in the first surface layer will form V_k centers, and the highly excited projectiles (also produced during RN) become relaxed by Auger de-excitation and autoionization processes, leading to electron emission. If a projectile penetrates the surface layer still in an ionized or highly excited state, interatomic AN and RN will take place and further neutralize and/or de-excite the projectile, producing further electron-hole pairs. In this case "hot holes" will be formed with higher probability because of the higher electron density of states in the center of the valence band [21]. At low impact energy all defects are created in the near surface region, and diffusion processes are of minor importance.

The whole situation is similar to ESD where decay of electron-hole pairs into H and F centers followed by desorption of F^0 (and at elevated temperature also Li^0, see above) takes place. However, in contrast to ESD for ion impact no lithium overlayer could be observed, because down to the lowest impact energies sufficient momentum transfer is being provided by the projectiles for removing single, rather weakly (van der Waals) bound Li atoms from the LiF surface, even at room temperature. Therefore, stoichiometric desorption can be assumed for MCI impact, whereas for electron bombardment a Li enriched surface will be produced because only halogen atoms are emitted.

A special case is given for sputtering by singly charged Ar^+ ions. The respective yield stays constant at about 0.5 LiF molecules per ion (cf. Fig. 1) down to the lowest impact energy of 5 eV. "Coulomb explosion" as proposed by Bitenskii, Murakhmetov, and Parilis [5] can be excluded as sputter mechanism because it would produce nonthermal sputtered particles, in contrast to measurements showing that the emitted neutrals are mainly thermal [9] as for ESD. In addition, production of F^+ would be necessary for providing a sufficiently large repulsion between Li^+ and F^+ ions at the surface, but is not possible below 150 eV impact energy. Only one hole can be created via RN, but no electron. Therefore we have to assume that electrons are already available to a certain extent at thin polycrystalline LiF films [21]. Faster ions will penetrate increasingly deeper into the target, and electron-hole pair production may be supported by the ion's kinetic energy in a similar way as for "stimulated potential electron emission" from alkali halides [22]. For higher projectile potential energy a second neutralization channel will become active, as first observed for impact of slow He^+ on LiF [1], where the total sputter yield also stayed constant at low impact energy, but was slightly higher than for Ar^+ impact. If the potential energy is larger than twice the band gap of LiF (12 eV [18]), AN can take place near the surface, forming two holes and one electron, as apparent from F^+ desorption from LiF [23].

Multicharged ions will produce an accordingly larger number of holes in the LiF valence band via RN above the surface, quasiresonant neutralization below the surface, and AN both above and below the surface, respectively, depending on the available total potential energy. At the same time, according to the available potential energy, electrons will also be excited and emitted [16].

At low MCI impact energies, we have applied a correction for possible image charge acceleration of the projectile. For this purpose, the respective formula for metallic surfaces [15,17] has been modified for both the larger work function and a finite dielectric permittivity of LiF, despite our unsatisfactory understanding of image charge formation for an alkali halide surface [19]. However, in this way, determined "effective" impact energies led to a practically linear relationship between the potential MCI energy and the corresponding total sputter yield, as shown in Fig. 2. Increase of the MCI impact energy will enhance the efficiency of hole formation in a similar way as for the singly charged ions. Slow MCI-induced electron emission is related to the MCI potential energy [16] in a similar way as the "potential sputtering" discussed here, with one important difference.

Increase of the Ar^{q+} charge from eight to nine produces one L-shell vacancy in the projectile. As first shown for MCI-induced electron emission from clean tungsten [24], the MCI-induced electron yield does not follow the relatively large jump in ion potential energy, but rather "saturates" because a major share of the additional potential energy will then be used up for producing a fast (ca. 200 eV) Auger electron during recombination of the Ar^{9+} L-shell vacancy [16]. On the other hand, the total yield for "potential sputtering" of LiF rises farther on more or less linearly with the projectile potential energy (cf. Fig. 2).

Figure 3 shows that one 200 eV electron can remove about 1.5 F^0 atoms from LiF, a figure which should become still higher if we consider secondary electron emission by the just discussed fast Auger electrons inside the LiF bulk. No Li surface layer as observed for ESD will be formed (see above). Consequently, the more or less linear relationship between the potential energy of projectile ions and the total sputter yield also stays on for Ar^{9+}.

Finally, Fig. 3 makes clear that ESD due to the rather slow electrons (typically $\leq$10 eV) which constitute the bulk of MCI-induced electron emission [15], cannot cause a major contribution to the here discussed "potential sputtering" process.

In conclusion, absolute total sputter yields have been measured for impact of MCI on LiF at such low impact energies where the projectile potential energy provided for the dominant part of energy transfer to the surface. These sputter yields are composed of more than 99% neutral particles [25], and they result primarily from decay of electron-hole pairs created in the LiF near surface region by electron capture to the multicharged ions. Up to the highest charge state ($q = 9$) involved in this study, no evidence for a strong influence of the so-called Coulomb explosion mechanism on the total sputter yield could be found.

This work was financially supported by Austrian Fonds zur Förderung der Wissenschaftlichen Forschung and carried out within the Human Capital and Mobility Network "Interaction of Slow Highly Charged Ions with Solid Surfaces" of the European Union.

*To whom correspondence should be addressed. Electronic address: varga@eapv38.tuwien.ac.at.

[1] T. Neidhart *et al.*, Nucl. Instrum. Methods Phys. Res., Sect. B **90**, 496 (1994).
[2] P. Varga and U. Diebold, in *Low Energy Ion-Surface Interaction,* edited by J. W. Rabalais (Wiley, New York, 1994).
[3] S. Radzhabov, R. Rakhimov, and P. Abdusalumov, Izv. Akad. Nauk SSSR, Ser. Fiz. **40**, 2543 (1976).
[4] S. Radzhabov and R. Rakhimov, Izv. Akad. Nauk SSSR, Ser. Fiz. **49**, 1812 (1985), [Bull. Acad. Sci. USSR, Phys. Ser. **49**, 141 (1985)].
[5] I. S. Bitenskii, M. N. Murakhmetov, and E. S. Parilis, Sov. Phys. Tech. Phys. **24**, 618 (1979).
[6] W. Eckstein *et al.*, Report No. IPP 9/82, Max Planck Institut für Plasmaphysik, 1992.
[7] M. Szymonski, in *Proceedings of SPUT 92*, edited by P. Sigmund (The Royal Academy of Sciences and Letters, Copenhagen, 1993) and references therein.
[8] M Szymonski *et al.*, Surf. Sci. **260**, 295 (1992); N. Siefert *et al.*, Phys. Rev. B **47**, 7653 (1993); R. Walkup, P. Avouris, and A. Ghosh Phys. Rev. B **36**, 4577 (1987); T. Green *et al.*, Phys. Rev. B **35**, 781 (1987).
[9] Z. Postawa *et al.*, J. Chem. Phys. **96**, 3298 (1992).
[10] Crystallographic orientation *(YXwl)* +21.93°, −33.93° as defined in *IEEE Standard on Piezoelectricity (Std. 176-1978)* (IEEE, New York, 1978).
[11] M. Leitner *et al.*, Rev. Sci. Instrum. **65**, 1091 (1994).
[12] R. Montereali *et al.*, Thin Solid Films **196**, 75 (1991).
[13] T. Neidhart *et al.*, Nucl. Instrum. Methods Phys. Res., Sect. B (to be published).
[14] P. Varga and H. Winter, in *Particle Induced Electron Emission II,* edited by G. Höhler, Springer Tracts in Modern Physics Vol. 123 (Springer, Berlin, 1992).
[15] F. Aumayr and HP. Winter, Comments At. Mol. Phys. **29**, 275 (1994), and references therein.
[16] M. Vana *et al.*, Europhys. Lett. **29**, 55 (1995).
[17] P. Burgdörfer, in *Review of Fundamental Processes and Applications of Atoms and Ions,* edited by C. D. Lin (World Scientific, Singapore, 1993), Chap. 11.
[18] B. Kunz, Phys. Rev. B **26**, 2056 (1981).
[19] H. Limburg *et al.* (to be published).
[20] R. Williams *et al.*, Phys. Rev. B **33**, 7232 (1986); R. Williams and K. Song, J. Phys. Chem. Solids **51**, 679 (1990).
[21] N. Siefert *et al.*, Nucl. Instrum. Mehods Phys. Res., Sect. B (to be published); N. Siefert *et al.*, Phys. Rev. B **51**, 12 202 (1995).
[22] R. Rakhimov and S. Gaipov, Izv. Akad. Nauk SSSR, Ser. Fiz. **43**, 1894 (1979).
[23] P. Varga, U. Diebold, and D. Wutte, Nucl. Instrum. Methods Phys. Res., Sect. B **32**, 331 (1988).
[24] M. Delauney *et al.*, Phys. Rev. B **35**, 4232 (1987).
[25] T. Neidhart *et al.*, Nucl. Instrum. Methods Phys. Res., Sect. B (to be published).